

# Wall-to-bed mass transfer in three phase fluidized beds in the presence of angled disc promoter

P. Rohini Kumar<sup>1</sup> · K. Ashok Kumar<sup>2</sup> · M. S. N. Murty<sup>3</sup> · K. V. Ramesh<sup>2</sup> 

Received: 23 February 2016 / Accepted: 27 April 2017 / Published online: 8 May 2017  
© Springer-Verlag Berlin Heidelberg 2017

**Abstract** Mass transfer coefficient data were computed from measured limiting current values obtained at point electrodes fixed flush with the inner wall of an outer cylinder of three phase fluidized bed electrochemical reactor in the presence of an angled disc internal. Nitrogen was used as gas phase. Glass balls of different diameters were used as solid phase. The liquid phase was an electrolyte that belonged to the ferricyanide-ferrocyanide redox system. Enhancement in mass transfer coefficient obtained in the case of three-phase fluidized bed in the presence of angled disc internal was upto 14 fold in comparison with the homogeneous flow of electrolyte in plain pipe. The mass transfer coefficient data thus obtained were found to increase with increasing gas velocity, pitch and disc diameter. An increase in disc angle resulted in a decrease in the mass transfer coefficient. The influence of liquid velocity, promoter rod diameter and particle diameter on mass transfer coefficient was found to be insignificant. The entire mass transfer coefficient data obtained in the present study were subjected to regression analysis and useful correlation equation was obtained.

**Keywords** Mass transfer coefficient · Turbulent promoter · Inclined disc · Angled disc · Electrochemical cell · Three phase fluidized bed

## Nomenclature

A	area of the reacting surface	[m <sup>2</sup> ]
C	Constant	[-]
C <sub>0</sub>	concentration of reacting ion (Fe <sup>2+</sup> or Fe <sup>3+</sup> )	[kmol/m <sup>3</sup> ]
D <sub>L</sub>	diffusivity of reacting species	[m]
d <sub>p</sub>	particle diameter	[m]
d <sub>k</sub>	disc diameter	[m]
d <sub>r</sub>	rod diameter	[m]
F	Faraday constant	[C/ kmol]
g	acceleration due to gravity	[m/s <sup>2</sup> ]
H	height of test-section/height of the fluidized bed	[m]
i <sub>L</sub>	limiting current	[A]
k <sub>L</sub>	mass transfer coefficient	[m/s]
n	number of electrons released or consumed during the reaction	[-]
p	pitch or disc spacing	[m]
U <sub>g</sub>	superficial gas velocity	[m/s]
U <sub>L</sub>	superficial liquid velocity	[m/s]
w	width of tape	[m]
X	longitudinal distance	[m]

## Greek Letters

μ <sub>L</sub>	liquid viscosity	[kg/m s]
ρ <sub>L</sub>	liquid density	[kg/m <sup>3</sup> ]
θ	disc angle	[degrees]

## Dimensionless groups

j <sub>D</sub>	Coulburn j-factor = $\frac{k_L}{U_L} Sc^{2/3}$
Re <sub>p</sub>	Reynolds number based on particle diameter = $\frac{\rho_L d_p U_L}{\mu_L}$
Sc	Schmidt number = $\frac{\mu}{\rho D_L}$

## 1 Introduction

Three-phase fluidized beds offer many advantages. High macromixing, large longitudinal dispersion of phases, high

✉ K. V. Ramesh  
kvramesh69@yahoo.com

<sup>1</sup> Department of Chemical Engineering, RVR & JCCOE, Guntur 522019, India

<sup>2</sup> Department of Chemical Engineering, Andhra University, Visakhapatnam 530003, India

<sup>3</sup> Department of Chemical Engineering, GVPCOE(A), Visakhapatnam 530048, India

reactant conversions, uniform temperature, better temperature controllability, magnitudes of augmentation in heat transfer rates, ease in replacement of catalyst, good controllability of catalyst activity, minimum flow misdistribution etc., are some advantages that made the three-phase fluidized beds attractive for process industry applications [1]. Application of three-phase fluidization to electrochemical processes gained attention in recent times. Investigations in using a rectangular electrochemical cell [2], annular conduits [3, 4], cross-flow elements [5], helicoidal tape promoter [6], twisted tape [7] and disc promoter [8] were only few studies taken up in this direction.

In so many cases, presence of internals such as draft tubes, baffles, immersed heaters, geometrical irregularities etc., occur for obvious reasons. Sometimes to achieve improved heat and mass transfer rates, turbulent promoters are purposefully used. Thus the usage of internal elements becomes necessary in many applications. Arrangement of an internal in the three-phase fluidized bed electrochemical reactor highly increases the complexity of the hydrodynamic and transport phenomena. Literature survey revealed that only few studies were taken up earlier in this direction that reported the systematic effects of the geometry of the internal elements on mass transfer [5–8].

Investigations were carried out on using disc promoter elements for enhancement of wall-liquid mass transfer in homogeneous flow [9], in liquid fluidized beds [10], in gas-liquid upflow bubble columns [11] and in gas-liquid-solid fluidized beds [8]. It was observed that the mass transfer coefficient exhibited fluctuations in the axial direction in these cases in the presence of disc promoter and these fluctuations were upto 90% from the mean value [8–11]. However, Niranjana Rao et al. [12, 13] and Ramaprasad et al. [14] reported nearly uniform mass transfer coefficient values in the longitudinal direction in the presence of angled disc promoter in homogeneous flow, liquid fluidized bed and gas-liquid upflow bubble columns respectively. Although disc promoter is superior in yielding high mass transfer coefficient values, the disadvantage of realizing non uniform mass transfer coefficient in the axial direction could be overcome by angled discs. Alemrajabi and Moradi [15] investigated the effect of angled discs on heat transfer in a tube of constant wall temperature. Kumar and Roy [16] studied the effect of inclination of discs on fluidized bed behavior in a gas-solid fluidized bed. These studies revealed that the angled disc promoter element is promising in obtaining magnitudes of improvements in mass transfer coefficients. Also it was found that no study has been reported on wall-to-bed mass transfer in a three-phase fluidized bed with angled disc promoter internal.

In view of this, the present investigation has been carried out by the authors to study the effect of pertinent dynamic and geometric variables on mass transfer coefficient in a three-phase fluidized bed in the presence of angled disc promoter elements. The flow system chosen consisted of nitrogen as gas phase, liquid electrolyte belonging to ferricyanide-

ferricyanide redox system as liquid phase and glass balls as solid phase. Limiting current technique has been used to obtain mass transfer coefficient data. The range of variables covered in the present study are compiled and shown in Table 1.

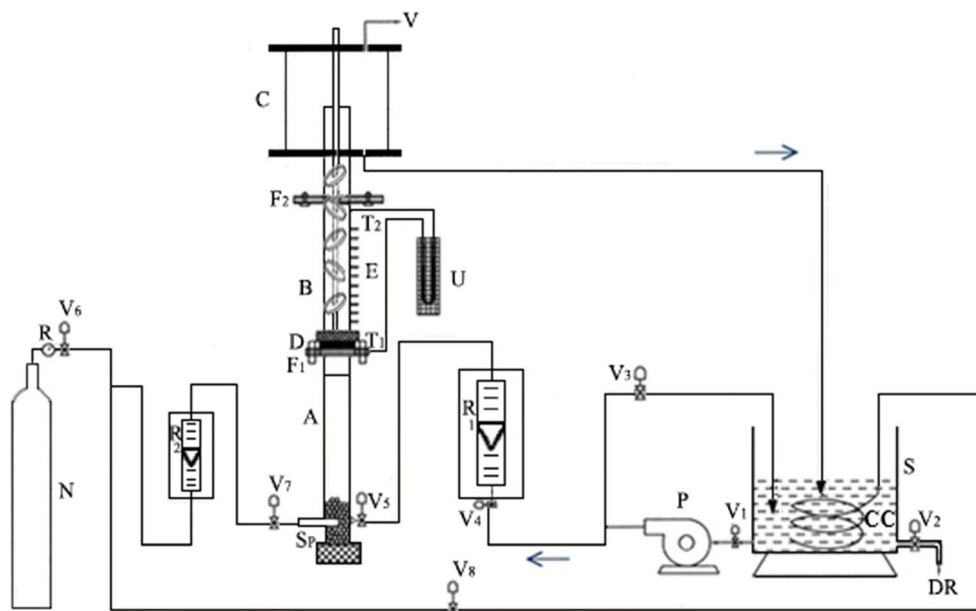
## 2 Experimental

The schematic diagram of the experimental test rig employed in the present investigation is shown depicted in Fig. 1. It consists of a 100 l capacity storage tank (S) of Sintex make. This tank is usually filled with 80 l of liquid electrolyte. A copper spiral coil (CC) containing small perforations is immersed in this electrolyte. Nitrogen gas is supplied to this coil so that the gas escapes from the perforations and rises through the liquid electrolyte causing deaeration of the liquid electrolyte. Deaeration by nitrogen removes the traces of oxygen that is present in the liquid electrolyte. Supply of nitrogen gas to this spiral coil is made from nitrogen gas cylinder (N) and controlled using valve  $V_8$ . Provision for draining of liquid electrolyte from the storage tank is arranged by connecting drain section (DR) which is operated using valve  $V_1$ . This arrangement helps in periodic cleaning of the tank. A stainless steel pump (P) of Kirloskar make having 1 kW rating is used for circulating the liquid electrolyte in the experimental unit. The pump suction is connected to the storage tank with a pipeline having a valve  $V_2$ . The discharge section of the pump has two branches. One branch is used as a by-pass line that is equipped with valve  $V_3$ . Another branch is connected to the inlet of rotameter  $R_1$  along with valve  $V_4$ . This rotameter is of Indus make and has been calibrated upto 60 l per minute using the fluid electrolyte. The outlet of  $R_1$  is connected to the inlet arm of experimental column which is also equipped with a globe valve  $V_5$  that helps in controlling flow rate of liquid into the experimental column. Analytical reagent grade nitrogen gas is procured from Bharat Oxygen Corporation, Visakhapatnam, India, in high pressure cylinders. This cylinder is fixed with a gas regulator of Concoa make (France) with

**Table 1** Range of variables

S. No.	Parameter	Minimum	Maximum
1	Diameter of column [cm]	6.73	-
2	Diameter of the rod, $d_r$ [cm]	0.6	1.3
3	Pitch, $p$ [cm]	3.0	10.0
4	Disc diameter, $d_K$ [cm]	3.0	6.0
5	Particle diameter, $d_p$ [cm]	0.293	0.562
6	Angle of the disc, $\theta$ [degrees]	0	67.5
7	Velocity of liquid, $U_L$ [m/s]	0.04	0.28
8	Velocity of gas, $U_g$ [m/s]	0.014	0.070
9	Reynolds number, $Re$	3598	22,236
10	Particle Reynolds number, $Re$	266	1852

**Fig. 1** Schematic diagram of the experimental unit. A - entrance calming section; B - test section; C - exit section; CC - copper coil; D - distributor wire mesh; DR - drain; E - electrodes; F<sub>1</sub>, F<sub>2</sub> - flanges; N - nitrogen cylinder; P - pump; R - Regulator, R<sub>1</sub> and R<sub>2</sub> - rotameters; S - storage tank; T<sub>1</sub>, T<sub>2</sub> - pressure tapings, U - manometer; V - vent; V<sub>1</sub> to V<sub>8</sub> - valves



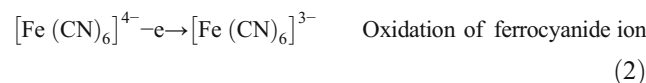
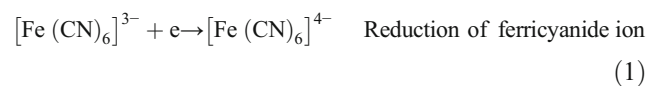
Model no. 316 L. The outlet flow of nitrogen was divided into two lines: one line is used to supply nitrogen into spiral coil (CC) for deaeration of liquid electrolyte and another line is passed through rotameter R<sub>2</sub>, the exit point of which is connected to the bottom portion of experimental column for admitting nitrogen gas into the experimental column. Valves V<sub>6</sub> and V<sub>7</sub> are useful in regulating the nitrogen gas flow into experimental column. Rotameter R<sub>2</sub> is of Indus make and has a precalibrated range of zero to 30 l per minute. For even distribution of gas in the experimental column, the nitrogen gas is passed through a sparger (Sp). Since the liquid entry into the experimental column is tangential, the bottom part of the experimental column is filled with marble stones. The presence of marble stones in the entry point helps in eliminating the tangential entry effects.

The experimental column shown in Fig. 1 consisted of three sections: an entrance calming section (A), a test section (B) and an exit section (C). The entrance calming section (A) is made of a copper tube of 6.73 cm inner diameter, outer diameter of 7.62 cm and 1.07 m long. This section is connected to the main test section (B) by means of a flange (F<sub>1</sub>). The test section (B), which is the electrochemical cell, is made of smooth perspex tube of 6.73 cm inner diameter and 0.6 m height. The inner wall of the test section is equipped with copper point electrodes 34 in number each having a diameter of 3.42 mm. One end of these electrodes is fixed flush with inner surface of the test section while the other end projected outward served as terminal for connecting the electrodes to the external electric circuit. A stainless steel wire mesh (D) is placed at the bottom of the test section. This serves as a support to the bed of solids and also facilitates uniform distribution of both electrolyte and gas in the test section. The exit section (C) is connected to the test section with a flange (F<sub>2</sub>).

This section is also of the same inner diameter as A and B, with its top end open into the atmosphere and hence acts essentially as a gas-liquid separator. The electrolyte is drained into the storage tank from the bottom of the separator and nitrogen gas leaves into the atmosphere through vent (V).

The angled disc promoter comprises of an array of uniform diameter discs fixed at a specified inclination and equal spacing on a copper rod as shown in Fig. 2. This promoter element is arranged coaxially in the test section and exit calming section. The promoter elements of different geometric characteristics (viz., diameter of rod  $d_r$ , pitch  $p$ , diameter of the angled disc  $d_k$  and angle of disc  $\theta$ ) were fabricated and used in the present studies. The diameters of the glass balls used as bed material in the present study are 2.93 mm, 4.24 mm, 5.62 mm.

Potassium ferrocyanide, potassium ferricyanide and sodium hydroxide were added to distilled water in required quantities so that the resulting solution would have their normalities as 0.01, 0.01 and 0.5 respectively. This solution is used as liquid electrolyte in the present study. The limiting current is measured at copper point electrodes fixed flush with inner wall of the outer cylinder in the test section. The limiting current is measured for reduction of ferricyanide ion and oxidation of ferrocyanide ion. The electrode reactions involved in this study are:



From the measured limiting current value ( $i_L$ ) at any given electrode, the mass transfer coefficient was calculated using

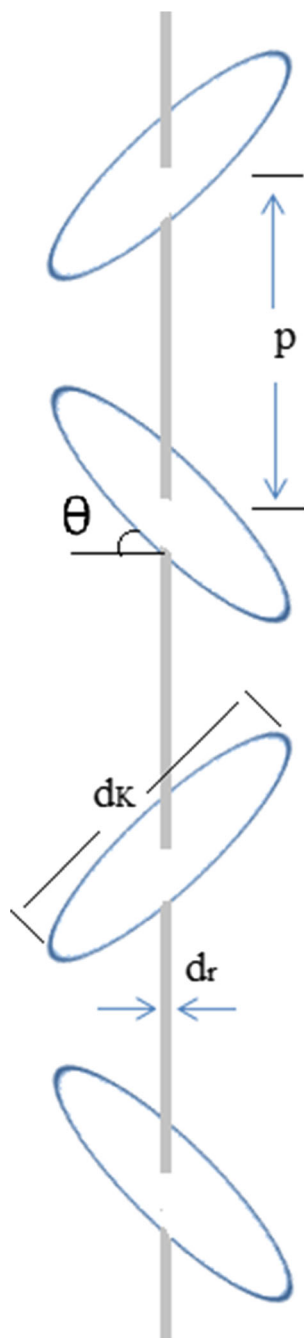


**Fig. 2** Details of angled disc promoter.  $d_r$  = rod diameter;  $d_k$  = disc diameter;  $p$  = pitch;  $\theta$  = angle

the following eq. [17].

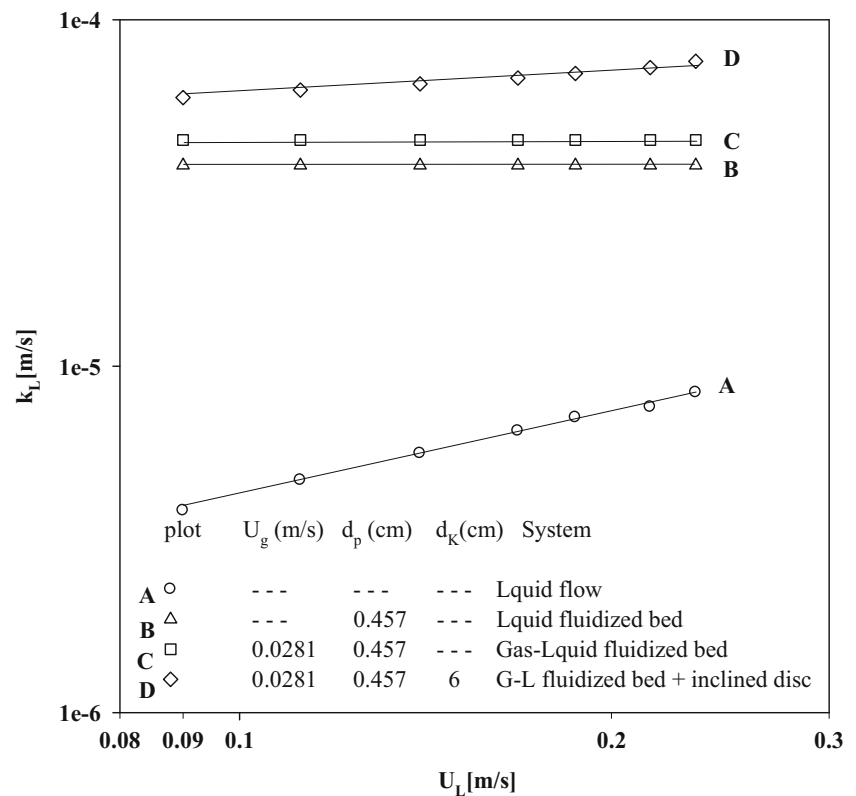
$$k_L = \frac{i_L}{zAFC_0} \quad (3)$$

Gas holdup is computed from measured pressure drop. Solids holdup and bed porosity are obtained from bed height measurements. Liquid holdup is obtained by subtracting gas and solid holdups from unity. Niranjana Rao et al. [19] reported the phase holdup data in a three-phase fluidized bed in the presence of angled disc promoter.

### 3 Results and discussion

Prior to the commencement of mass transfer studies in three-phase fluidized bed with angled disc promoter, few experiments were carried out initially to verify the reproducibility of earlier published data and also to realize the extent of augmentation that can be expected in the present study. These data were shown plotted in Fig. 3. Four cases have been considered: (i) homogeneous flow (plot A), (ii) liquid fluidized bed (plot B), (iii) gas-liquid fluidized bed (plot C) and (iv) gas-liquid fluidized bed with angled disc promoter (plot D). Plot A shows the mass transfer coefficient data predicted from Lin et al. [17] for the case of homogeneous flow of fluid electrolyte. The mass transfer coefficient data obtained for the case of liquid-solid fluidized bed were found to be in accordance with that of Jagannatha Raju and Venkata Rao [18] and were shown as plot B. Similarly the mass transfer coefficient data obtained for the case of three-phase fluidized bed were in accordance with Ramesh et al. [6] and shown in plot C. Plot D shows the present mass transfer coefficient data with angled disc promoter in three-phase fluidized beds. The magnitudes of improvements in mass transfer coefficient values over homogeneous liquid flow were shown through plots B, C and D. Plots A and B show that the improvements in the mass transfer coefficient due to presence of fluidizing solids were up to a maximum of 9 fold. The reasons for this behavior can be outlined in the following sentences. It is well established that the main resistance to the transfer process is offered by the fluid film that present on the reacting surface. If the thickness of this film is more, then the resistance for diffusion is more. In homogeneous flow, the film thickness is essentially influenced by the eddies present in the flowing fluid if the flow is turbulent. In case of liquid-solid fluidized beds, the solid particles are essentially suspended in the flowing liquid by virtue of the momentum of the liquid. These fluidizing particles generate severe scouring action that leads to striking of the resistance film on the transfer surface. Hence the thickness of the resistance film gets reduced thus yielding increased mass transfer coefficients.

The improvements due to the introduction of gas phase into the liquid-solid fluidized bed were up to 20% (Plots B and C). The addition of gas phase generates severe churning action as the gas bubbles owing to high density difference move at high velocities in the upward direction creating intense churning action. This further reduces the film thickness causing further increase in mass transfer coefficients. Although one cannot expect multifold increase in  $k_L$  values due to the introduction of gas into the liquid fluidized beds, definitely it can be expected that additional turbulence is imparted, yielding enhanced  $k_L$  values in gas-liquid fluidized bed (Plot C). The introduction of gas in liquid fluidized bed decreases the minimum liquid fluidization velocity and also maintains the fluidized bed status even in the lean bed region. Therefore, constant  $k_L$  values can be expected over wider range of liquid

**Fig. 3** Comparison of  $k_L$  values in different flow systems

velocities in three-phase fluidized beds in comparison with two-phase fluidized beds. Further, presence of inclined disc promoter in three-phase fluidized beds results in enhanced mass transfer coefficient as revealed by plots D and C. The presence of an internal in the test section reduces the hydraulic diameter hence the flow velocities of the fluids will be much higher than the superficial velocities. If the flow path thus created is in favor of reducing the thickness of the resistance film, then highest mass transfer coefficient can be realized due to the combined effect of all these. Plot D gives the magnitudes of augmentation in mass transfer coefficient in three-phase fluidized bed due to the introduction of angled disc promoter were upto 33% in lower liquid velocity end and 70% in higher liquid velocity end (Plots C and D). The plots reveal that highest mass transfer coefficient could be realized in a three-phase fluidized bed with the angled disc promoter. Presence of promoter in a three-phase fluidized bed was found to show an augmentation in the mass transfer coefficient upto a maximum of 15 fold over that of homogeneous flow (plots D and A). These observations indicate that the introduction of gas and angled disc promoter into a liquid-solid fluidized bed (Plot B) is definitely advantageous as their combined effect enhances turbulence resulting in increased mass transfer. Augmentation of the mass transfer coefficient at the wall electrodes is attributed to the effective reduction in the boundary layer thickness due to the prevailing tractive shear at the electrode surface. The combined effect of fluidizing solids, gas bubble flow and angled disc promoter would contribute

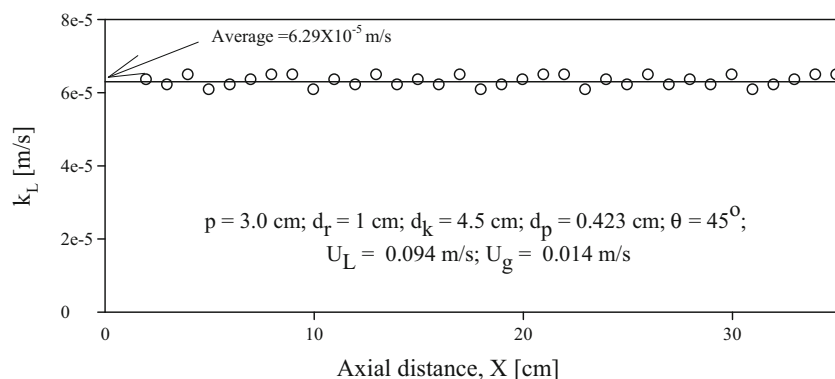
towards the effective reduction in the boundary layer thickness considerably.

### 3.1 Longitudinal variation of limiting current

Previous studies on mass transfer coefficient employing angled disc promoter in homogeneous flow [12], liquid-fluidized beds [13] and gas-liquid upflow bubble columns [14] reported that the existence of fluctuations in mass transfer coefficient along the axial direction but these fluctuations are not that significant. Therefore, in the present study investigations were conducted to ascertain whether axial variation of mass transfer coefficient exists or does not exist in the three-phase fluidized bed electrochemical reactors with angled disc promoter. The mass transfer coefficient data thus obtained have been presented in Fig. 4.

A close inspection of the plot of Fig. 4 reveals that there exists fluctuations in mass transfer coefficients in axial direction but their magnitudes are very small and they followed no specific trend. The reason can be attributed to the formation of asymmetrical wakes between two successive discs which rotate randomly in the test section. This leads to effective mixing of fluid elements in the axial direction also, thus causing nearly absence of axial variation of mass transfer coefficient. Thus the fluctuations in the mass transfer coefficient are essentially very small. Therefore, no significant variation of mass transfer coefficient along the longitudinal direction can be noticed in the presence of an angled disc promoter element in a three-

**Fig. 4** Longitudinal variation of mass transfer coefficient



phase fluidized bed. In view of this, all 34 electrodes were joined together and mass transfer coefficient for this combined electrode has been measured for all subsequent runs in the present experiment.

### 3.2 Effect of gas and liquid velocities on $k_L$

The mass transfer coefficient data in a three-phase fluidized bed in the presence of angled disc promoter  $\{p = 5.0 \text{ cm}, d_r = 1.0 \text{ cm}, d_k = 4.5 \text{ cm}, d_p = 4.24 \text{ mm}, \theta = 45^\circ\}$  for three superficial liquid velocities 0.093, 0.121 and 0.149 m/s were plotted against superficial gas velocity and shown in Fig. 5. A close examination of the plots of this figure revealed that the influence of liquid velocities on mass transfer coefficient appears to be marginal. It is understood that the total resistance to the mass transfer process lies in the fluid film that appears on the electrode surface. In flow systems that contain liquid alone, an increase in mass transfer coefficient was observed with increasing liquid velocity. This is due to increase in turbulence owing to increase in liquid velocity. Increase in turbulence makes the resistance film thin. Therefore high values of mass transfer coefficient would be realized. Addition of fluidizing particles strike the resistance film very strongly.

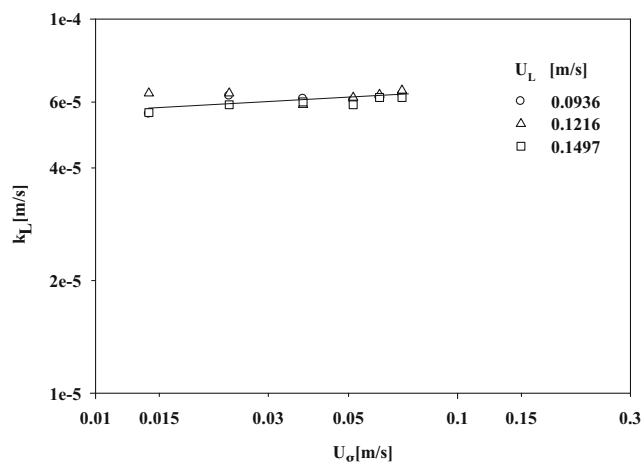


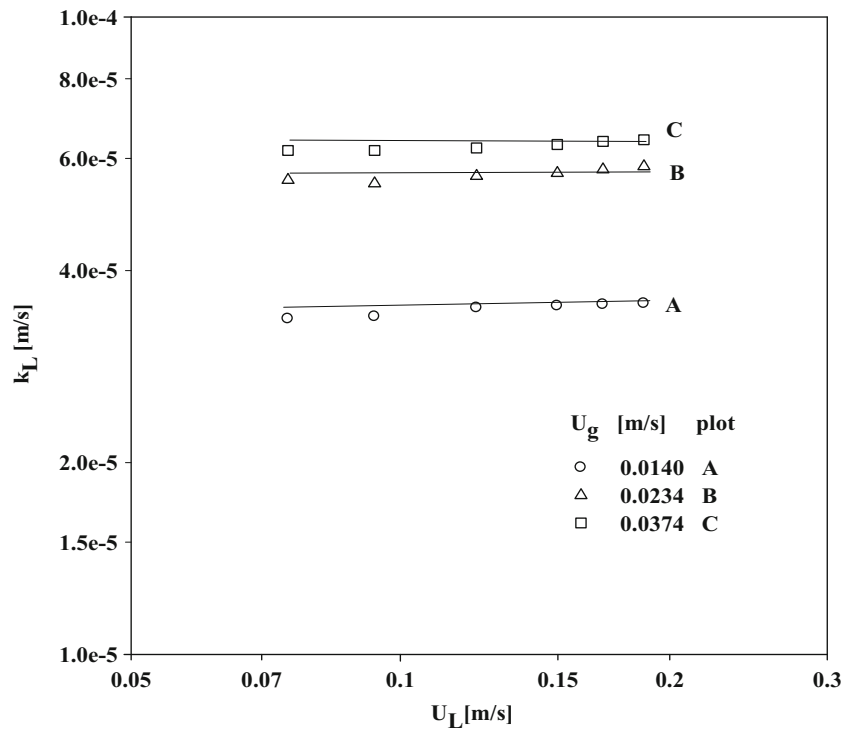
**Fig. 5** Variation of mass transfer coefficient ( $k_L$ ) with superficial gas velocity ( $U_g$ ) at constant  $\{p=5\text{cm}, d_r=1.0 \text{ cm}, d_k=4.5 \text{ cm}, d_p=4.243\text{mm}, \theta=45^\circ\}$

Hence the resistance film thickness decreases further. This leads to the realization of enhanced mass transfer coefficient values. However in the fluidizing regime, the mass transfer coefficient would be nearly constant and only at very high liquid velocities the mass transfer coefficient values start decreasing due to lean bed conditions. Introducing gas into liquid flow also renders the resistance film thin because of intense churning action generated by the bubble flow as seen in gas-liquid upflow bubble columns. In the present case the total turbulence that is generated is due to the combined effect of liquid velocity, gas velocity, fluidizing particles and internal element. Within the range of liquid velocity considered in the present study, when keeping all other parameters fixed, it seems there is no significant variation in the total turbulence and hence the mass transfer coefficient values are nearly unaffected. However, it can be anticipated that variation in gas velocity has reckonable influence on mass transfer coefficient because of severe scouring action generated by bubble flow. Therefore the mass transfer coefficient was found to be increasing with an increase in gas velocity as revealed from Fig. 6.

### 3.3 Effect of pitch on $k_L$

Figure 7 shows the mass transfer coefficient data plotted against liquid velocity for the case of angled disc promoter  $\{d_r = 0.6 \text{ cm}, d_k = 4.5 \text{ cm}, d_p = 4.243 \text{ mm}, \theta = 45^\circ\}$  when the gas velocity is maintained constant at 0.0327 m/s. An examination of the plots of this figure indicates that the pitch had significant influence on the mass transfer coefficient. An increase in pitch value resulted in an increase in mass transfer coefficient. The reason for this behavior can be explained like this. As the liquid which is the continuous phase in the present system, passes over the trailing edge of the inclined disc and the leading edge of the next inclined disc in the flow path of the fluid, formation of wakes occur which spread over the entire space between two successive discs. However, these wakes are not symmetric and hence they revolve around their axes which create severe churning action. Since the wakes form in the longitudinal direction spreading between two

**Fig. 6** Variation of mass transfer coefficient ( $k_L$ ) with superficial liquid velocity ( $U_L$ ) at constant  $\{p=5\text{cm}, d_r=1.0\text{ cm}, d_K=4.5\text{ cm}, d_p=4.243\text{mm}, \theta=45^\circ\}$



successive discs, as the pitch is increased, larger wakes formed, and these wakes generate intense churning action than smaller wakes. Thus, an increasing trend in mass transfer coefficient would be noticed with increasing pitch. The increasing trend is also evident from its inset Fig. 7a.

**3.4 Effect of disc diameter on  $k_L$**

The data on mass transfer coefficient plotted against liquid velocity for three different disc diameters viz., 3.0, 4.5 and 6.0 cm with the experimental conditions  $\{p = 5.0\text{ cm},$

$d_r = 1.0\text{ cm}, d_p = 4.24\text{ mm}, \theta = 45^\circ$  and  $U_g = 0.0327\text{ m/s}\}$  and shown in Fig. 8. An observation of the plots of this figure reveals that mass transfer coefficient increased with increasing disc diameter. As the disc diameter increases, the hydraulic mean diameter decreases, hence the flow velocities of the fluids increase. Further the width of the wake would be similar to the diameter of the disc. Therefore, larger the diameter of the disc, larger the volume and mass of the wake. Hence, at given conditions, an increase in disc diameter results in an increase in the wake momentum and also it leads to severe churning action resulting from the wakes. Hence, an increase

**Fig. 7** Variation of mass transfer coefficient with pitch at constant  $\{U_g=0.03276\text{ m/s}, d_r=0.6\text{ cm}, d_K=4.5\text{ cm}, d_p=4.243\text{ mm}, \theta=45^\circ\}$

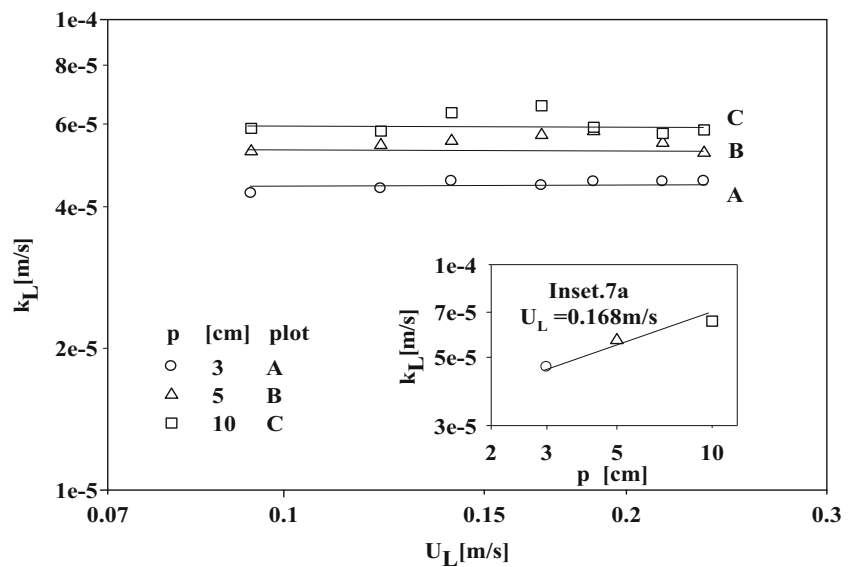
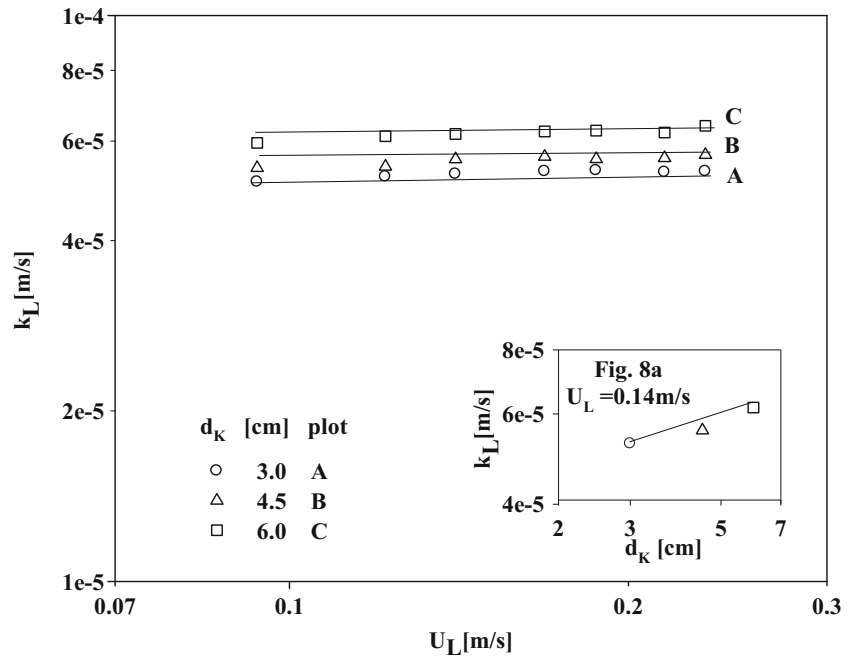


**Fig. 8** Variation of mass transfer coefficient with disc diameter at constant  $\{U_g=0.03276\text{m/s}, d_r=1.0\text{ cm}, p=5\text{ cm}, d_p=4.243\text{mm}, \theta=45^\circ\}$



in disc diameter causes an increase in mass transfer coefficient. This is also evident from its inset Fig. 8a.

### 3.5 Effect of promoter rod diameter on $k_L$

It is understood that the angled disc promoter that was aligned coaxially in the test section, essentially acts as bluff body. Further, normal to the flow direction. The projected area of the angled disc completely enmasks the central rod. Hence one can expect that the influence of rod diameter on  $k_L$  would

be marginal. The observations made in the present study also revealed the same trends (graphs not shown).

### 3.6 Effect of disc angle on $k_L$

The data on mass transfer coefficient were plotted against liquid velocity for four angled discs with inclinations of 0, 22.5, 45 and 67.5 degrees for the case of  $\{p=5.0\text{ cm}, d_r=1.0\text{ cm}, d_K=4.5\text{ cm}, d_p=4.24\text{ mm}\}$  at  $U_g=0.0327\text{ m/s}$ , and the resulting graph was shown in Fig. 9. From an observation of the plots it can be found that the mass transfer

**Fig. 9** Variation of mass transfer coefficient with disc angle at constant  $\{U_g=0.0327\text{m/s}, d_r=1.0\text{ cm}, p=5\text{ cm}, d_K=4.5\text{ cm}, d_p=4.243\text{mm}\}$

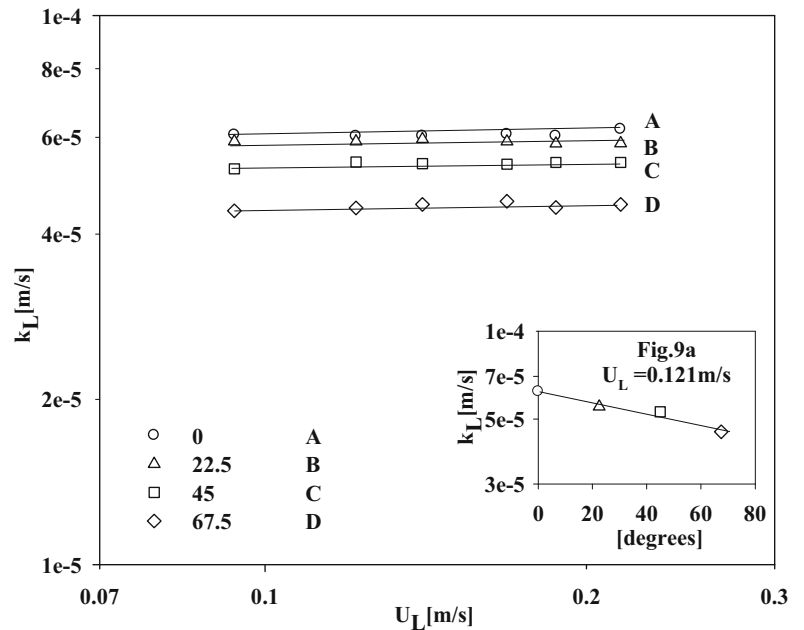
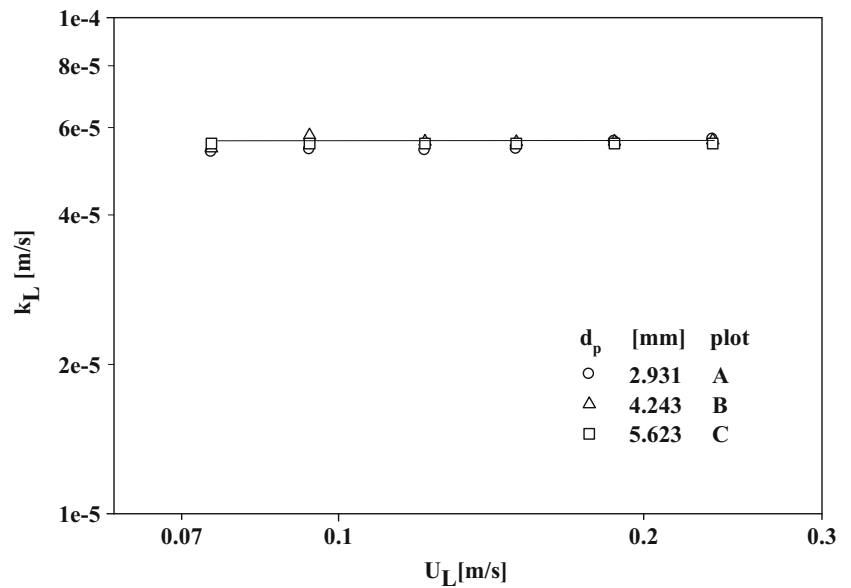




**Fig. 10** Variation of mass transfer coefficient with particle diameter at constant  $\{U_g=0.0234$  m/s,  $d_r=1.0$  cm,  $p=5$  cm,  $d_K=4.5$ cm,  $\theta=45^0\}$



coefficient decreased with increasing disc angle from 0 to 67.5 degrees. This observation is also conspicuous from the inset Fig. 9a. The reason for this can be explained in the following way. The disc essentially behaves as a bluff body. For a given disc diameter, when the angle is increased the projected area normal to the flow direction would decrease. Hence the obstruction area decreases, thus the flow velocities of the fluids would decrease with increase in disc inclination. Therefore, the mass transfer coefficient decreased.

### 3.7 Effect of particle diameter on $k_L$

The data on mass transfer coefficient obtained in the present case for three different particle diameters were plotted against superficial liquid velocity and shown presented in Fig. 10. The

experimental conditions employed for this study were  $\{p=5.0$  cm,  $d_r=1.0$  cm,  $d_K=4.5$  cm,  $U_L=0.121$  m/s,  $\theta=45^0\}$  and the diameters of the particles used were 2.93, 4.24 and 5.62 mm. A close examination of the plots of this figure revealed that the influence of particle size on mass transfer coefficient was found to be insignificant. Obeying this kind of trend can be reasoned as mentioned below. The contribution to the total turbulence in the present study is from liquid velocity, gas velocity, particle size, promoter geometry etc. By maintaining constant gas velocity, when the superficial liquid velocity is varied for three different particle sizes it seems there is no reckonable variation in the total turbulence. Hence, one can expect only marginal variation in the total turbulence and hence in mass transfer coefficient.

**Fig. 11** Correlation plot in accordance with eq. (8)

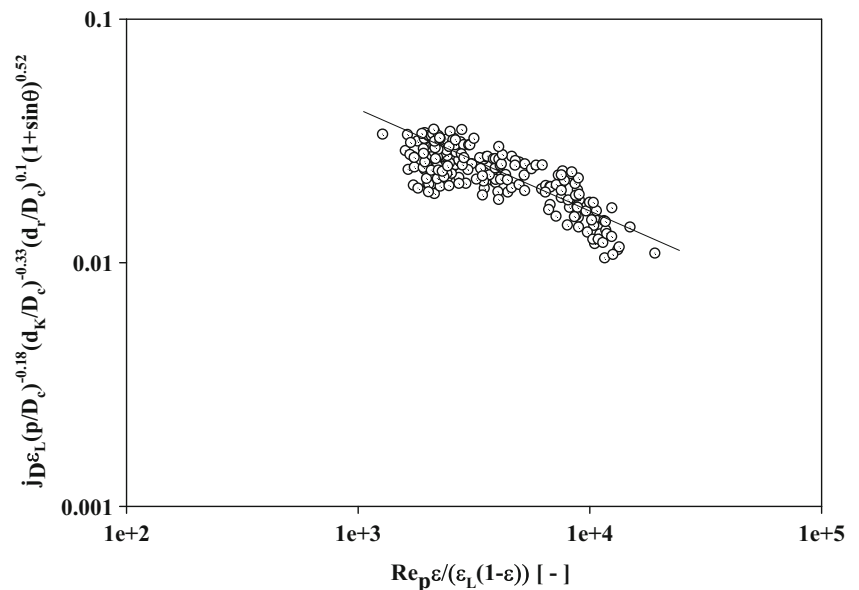
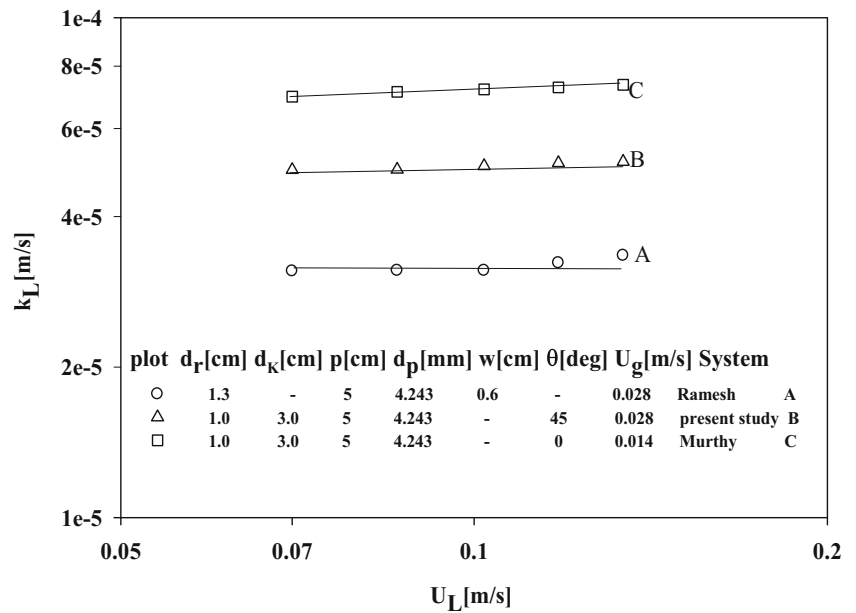


**Fig. 12** Comparison of results of the present study with those of earlier studies



**3.8 Development of generalized correlation on  $j_D \varepsilon_L$**

The discussion presented in sections 3.2 to 3.7 leads to the following functional relationship of the mass transfer coefficient with the variables of the present study as:

$$k_L = \Phi(U_L, U_g, p, d_r, d_K, d_p, \theta, D_c, \varepsilon_g, \varepsilon_L, \varepsilon, \varepsilon_s) \quad (4)$$

For the purpose of developing generalized correlations, the following functional relationship can now be assumed:

$$j_D \varepsilon_L = \frac{k_L \varepsilon_L}{U_L} Sc^{2/3} = [(\psi_1)^{n1} (\psi_2)^{n2} (\psi_3)^{n3} (\psi_4)^{n4} (\psi_5)^{n5}] \quad (5)$$

where,  $\psi_1 = \frac{d_e U_L \rho_L}{\mu_L} = Re$ .

Here  $d_e$  is the equivalent diameter. The actual velocity through the bed could be modified as  $U_L / \varepsilon_L$ . The equivalent diameter for a fluidized bed can be expressed in terms of particle diameter as  $d_p \varepsilon / (1 - \varepsilon)$ , where,  $\varepsilon$  = Bed voidage =  $\varepsilon_L + \varepsilon_g$ . Incorporating these factors in Re, the  $\psi_1$

can be modified as:

$$\psi_1 = \frac{d_p U_L \rho_L \varepsilon}{\mu_L \varepsilon_L (1 - \varepsilon)} = \frac{Re_p \varepsilon}{\varepsilon_L (1 - \varepsilon)}$$

$$\psi_2 = \frac{p}{D_C}$$

$$\psi_3 = \frac{d_K}{D_C}$$

$$\psi_4 = \frac{d_r}{D_C}$$

$$\psi_5 = 1 + \sin \theta$$

$\psi_2, \psi_3, \psi_4$  and  $\psi_5$  are the geometric ratios involving pertinent geometric variables. Also  $\psi_1$  is called as modified Reynolds number.

Now,

$$j_D \varepsilon_L = C \left( \frac{Re_p \varepsilon}{\varepsilon_L (1 - \varepsilon)} \right)^{n1} \left( \frac{p}{D_C} \right)^{n2} \left( \frac{d_K}{D_C} \right)^{n3} \left( \frac{d_r}{D_C} \right)^{n4} (1 + \sin \theta)^{n5} \quad (6)$$

**Table 2** Correlations proposed earlier for  $k_L$  in three-phase fluidized beds with internals

Investigators	Correlation	Eqn. no.	Promoter
Ramesh et al. [6]	$j_D \varepsilon_L = 0.14 \left[ \left( \frac{Re_p \varepsilon}{\varepsilon_L (1 - \varepsilon)} \right) \left( \frac{p}{D_C} \right) \right]^{-0.23}$	(9)	Helicoidal tape on a rod
Murty et al. [8]	$j_D \varepsilon_L = 0.03 \left( \frac{Re_p \varepsilon}{\varepsilon_L (1 - \varepsilon)} \right)^{-0.15} \left( \frac{p}{D_C} \right)^{-0.067} \left( \frac{d_K}{D_C} \right)^{0.89} \left( \frac{d_p}{D_C} \right)^{-0.6}$	(10)	String of discs
Subramanyam et al. [7]	$j_D = 59.37 Re_p^{-0.93} Fr_g^{0.04} \left( 1 + \frac{p}{D_C} \right)^{-0.41} \left( 1 + \frac{w}{D_C} \right)^{-0.54}$	(11)	Twisted tape

The entire data obtained in the present study on mass transfer coefficient are subjected to regression analysis yielding the following correlation equation:

$$j_{D\varepsilon_L} = 0.3336 \left( \frac{\text{Re}_p \varepsilon}{\varepsilon_L (1-\varepsilon)} \right)^{-0.294} \left( \frac{p}{D_C} \right)^{0.187} \left( \frac{d_K}{D_C} \right)^{0.339} \left( \frac{d_r}{D_C} \right)^{0.003} (1 + \sin\theta)^{-0.526} \quad (7)$$

Since the exponent on  $(d_r/D_C)$  is negligible, then this term can be taken as unity and can be removed from the correlation. By carrying out regression further yielded the following correlation equation:

$$j_{D\varepsilon_L} = 0.3336 \left( \frac{\text{Re}_p \varepsilon}{\varepsilon_L (1-\varepsilon)} \right)^{-0.294} \left( \frac{p}{D_C} \right)^{0.187} \left( \frac{d_K}{D_C} \right)^{0.339} (1 + \sin\theta)^{-0.526} \quad (8)$$

Average deviation = 16.92%; Standard deviation = 21.89%.

The correlation plot in accordance with eq. (8) has been shown in Fig. 11. Here modified Reynolds number is taken on x-axis and on y-axis  $Y$  is taken which is expressed as

$$Y = j_{D\varepsilon_L} \left( \frac{p}{D_C} \right)^{-0.187} \left( \frac{d_K}{D_C} \right)^{-0.339} (1 + \sin\theta)^{0.526}$$

### 3.9 Comparison of the results of the present study with those of earlier studies

The mass transfer coefficient data obtained in the present investigation in three-phase fluidized bed with the angled disc promoter were plotted (plot B) in Fig. 12. The mass transfer coefficient data of Ramesh et al. [6] obtained in three-phase fluidized bed in the presence of helicoidal tape promoter was shown as plot A for comparison. The mass transfer data of Murthy [8] obtained in three-phase fluidized bed in the presence of disc promoter was shown as plot C for comparison. A close observation of the plots of Fig. 12 reveals that the angled disc promoter had considerable influence on the mass transfer coefficient and higher mass transfer coefficient values could be realized in the presence of angled disc promoter in comparison with that of helicoidal tape internal (plots B and A), however, the disc promoter has yielded highest values (plot C). Realization of higher mass transfer coefficient values by using a string of discs as promoter internal is essentially due to its bluff nature. But it is well known that the disc promoter has the prime drawback of having high fluctuation in axial direction [8–11]. This disadvantage can be overcome by employing angled disc promoter. Hence it is obviously advantageous to use the angled disc promoter as an internal in three-phase fluidized beds,

Table 2 provides previously proposed correlations for wall-to-bed mass transfer coefficient in three-phase fluidized beds in the presence of different internals. A close inspection of these correlations reveals that previous investigators also obtained correlations containing Reynolds number and  $j_D$  factor, both modified for three-phase fluidized bed. The  $j_{D\varepsilon_L}$  was expressed as a function of this modified Reynolds number and other geometric variables expressed in dimensionless form. Eqns.(9) and (10) contained phase holdups also in the final correlation where as in the case of twisted tapes in eq.(11), the phase holdups were not considered.

## 4 Conclusions

- (i) The enhancement in mass transfer coefficient is about 14 times in three-phase fluidized bed with angled disc promoter in comparison with homogeneous flow.
- (ii) The mass transfer coefficient increased with gas velocity and the influence of liquid velocity on mass transfer coefficient was found to be insignificant.
- (iii) An increase in pitch and disc diameter resulted in an increase in mass transfer coefficient.
- (iv) The influence of rod diameter on mass transfer coefficient was found to be negligible.
- (v) The mass transfer coefficient decreased with increase in disc angle.
- (vi) The parametric effect of particle diameter on mass transfer coefficient was observed to be insignificant.

**Acknowledgements** The authors express their thanks to Late Mr. B. Niranjana Rao, Assistant Professor, Department of Chemical Engineering, GMR Institute of Technology, Rajam-532127, India, for his continuous help during experimentation.

## References

1. Fan L-S (1989) Gas-liquid-solid fluidization engineering. Butterworths, Stoneham
2. Morooka S, Kusakabe K, Kato Y (1980) Mass transfer coefficient at the wall of a rectangular fluidized bed for liquid-solid and gas-liquid-solid systems. *Int Chem Eng* 20:433–438
3. Yasunishi A, Fukuma M, Muroyama K (1988) Wall-to-liquid mass transfer in packed and fluidized beds with gas-liquid counter flow. *Journal of Chemical Engineering of Japan* 21:522–528
4. Ramesh KV, Raju GMJ, Bhaskara Sarma C, Murthy CVR, Subba Raju RV (2008) Liquid-wall mass transfer in three-phase fluidized beds with annular flow. *Indian Chemical Engineer* 50(4):277–287
5. Ramesh KV, Raju GMJ, Bhaskara Sarma C, Subba Raju RV (2008) Liquid-wall mass transfer in three phase fluidized beds with cross-flow of electrolyte. *Chem Eng J* 135:224–231
6. Ramesh KV, Raju GMJ, Murthy MSN, Bhaskara Sarma C (2009) Wall to bed mass transfer in three phase fluidized beds in the absence and presence of a composite promoter. *Chem Eng J* 152:207–211

7. Subramanyam BS, Murty MSN, Surendra Babu B, Ramesh KV (2014) Wall-to-bed mass transfer in a three-phase fluidized bed with twisted tape as internal. *Journal of The Institution of Engineers (India): Series E* 95(1):49–56
8. Murty MSN, Ramesh KV, Venkateswarlu P, Prabhakar G (2011) Ionic mass transfer in three-phase fluidized beds in the presence of disc promoters. *Chem Eng Commun* 198:1018–1032
9. Venkateswarlu P, Gopichand T, Jagannadha Raju GJV (2000) Increased mass transfer in a circular column in the presence of disc promoter *Journal of energy. Heat Mass Transf* 22:195–203
10. Ravi T, Srinivasa Rao B, Gopala Krishnna P, Venkateswarlu P (1996) Ionic mass transfer studies in fluidized beds with coaxially placed discs on a rod as internal. *Chem Eng Process* 35:187–193
11. Sarma GVS, Murty MSN, Ramesh KV, Raju GMJ (2011) Wall-to-bulk mass transfer in gas-liquid upflow bubble column with disc promoter. *Journal of Energy Heat and Mass Transfer* 33(3):233–249
12. Niranjana Rao B, Ramaprasad BSG, Murty MSN, Ramesh KV (2014) Mass transfer at the confining wall of an electrochemical cell in the presence of angled disc promoter. *American J Heat and Mass Transf* 1:113–129
13. Niranjana Rao, B., Rama Prasad, B.S.G., Murty, M.S.N., Ramesh, K.V (2015) Wall-to-bed mass transfer in a fluidized bed electrochemical reactor in the presence of angled disc promoter, AIChE spring meeting, April 27–30, Austin.
14. Rama Prasad BSG, Niranjana Rao B, Ashok Kumar K, Ramesh KV (2016) Mass transfer in a gas liquid upflow bubble column in the presence of angled disc promoter. *Chemical Technology: An Indian Journal* 11(5):1–9
15. Alemrajabi AA, Moradi GR (2007) Effect of inclined disks on heat transfer in a tube of constant wall temperature. *Heat Transf. Eng* 28: 1023–1031
16. Kumar A, Roy GK (2002) Minimum fluidization velocity in gas-solid fluidized beds with coaxial rod and disk promoters. *Indian Chem. Eng* 44:256–260
17. Lin CS, Denton EB, Gaskill HS, Putnan GL (1951) Diffusion controlled electrode reactions. *Ind Eng Chem* 43(9):2136–2143
18. Jagannadha Raju GJV, Venkata Rao C (1965) Ionic mass transfer in the presence of fluidized solids. *Indian J. Technol* 3:201–205
19. Niranjana Rao B, Murty MSN, Ramesh KV (2016) Phase holdups in a three-phase fluidized bed in the presence of an angled disc promoter. *Materials Today: Proceedings*, In Press.